Relaying System Based on Few-Mode EDFA for Space Division Multiplexing Wireless Optical Communication

Beibei Cui, Shanyong Cai, and Zhiguo Zhang

***Abstract*—Relay assisted transmission can compensate atmospheric turbulence, improve transmission distance, and realize communication between non-linear targets in free space optical communication (FSO) system. Space division multiplexing (SDM) greatly improves the channel capacity of FSO system. This paper focuses on the relay assisted transmission oriented to SDM wireless optical communication system. We develop a dual-hop SDM FSO communication model with two spatial mode channels. At the relay, the received optical signals are amplified by the few mode EDFA and forwarded to the destination. Simulation results show that the bit error rate (BER) of the dual-hop SDM system with a few mode EDFA based relay outperforms the single-hop SDM system. Under BER $= 1 \times 10^{-5}$, the power budget is increased by 0.53 dB, 1.2 dB, and 4.88 dB, when $C_n^2 = 4 \times 10^{-15}$, 7×10^{-15} and 1×10^{-14}, respectively. Moreover, the BER performance is the best when the relay is (originally in the middle of the link) slightly closer to the source.**

***Index Terms*—Few-mode EDFA, FSO, relay, space division multiplexing.**

I. Introduction

IN VIRTUE of its wide bandwidth and inherent security, free space optical (FSO) communication system has attracted much interest in recent years and is expected to be used in future integration network [1]. However, atmospheric channel fading, including atmospheric turbulence (AT) and beam broadening, limits the bit error rate (BER) performance and practical application of FSO system [2]. Therefore, many methods were proposed to suppress channel fading, such as error control coding [3], maximum-likelihood sequence detection (MLSD) [4], multiple-input multiple-output (MIMO) [5], and multi-hop relay assisted transmission [6]. Among them, relay assisted transmission is a simple and effective scheme and can realize communication between non-linear targets to avoid interruption caused by obstacles. At present, relay assisted transmission system based on photoelectric conversion and all-optical amplification has been studied. In [6], optical-to-electrical (OE) and electrical-to-optical (EO) convertors are employed at the relay, the improvement of power budget of this relaying system was discussed under different signal processing modes for the FSO communication system. Kazemlou et al. further discussed less complex all-optical relay assisted FSO system based on single-mode EDFA [7]. Moreover, M. A. Kashani et al. studied the effect of relay placement on BER in [8]. They pointed out that the best BER performance can be achieved when the relays are equally spaced for multi-hop link. While for parallel relay links, relays should be placed close to the source.

By transmitting multiple spatial modes in parallel, space division multiplexing (SDM) communication system can greatly improve the channel capacity. SDM related devices have developed rapidly. Neng Bai et al. fabricated multimode EDFA and few-mode EDFA (FM-EDFA) in 2011 and 2012 respectively [9], [10]. Then, using FM-EDFA as relay amplification for SDM optical fiber transmission system was generously studied [11]. For wireless optical communication system, researchers from the University of Central Florida firstly applied the FM-EDFA to the receiver of FSO system at the ECOC 2017 [12]. In 2019, we applied FM-EDFA to relay assisted transmission FSO system [13]. So far, the relaying system oriented to SDM FSO system is not fully characterized.

In this paper, FM-EDFA based all-optical relay are applied to short-reach (hundred meters) SDM FSO system. Dual-hop and single-hop SDM FSO system models are proposed. BER performance is numerically calculated. Results show that the dual-hop system with a FM-EDFA based relay outperforms the single-hop system, mainly because the FM-EDFA can reduce turbulence-induced crosstalk among modes.

II. System and Channel Model

A. System Model

The system model of dual-hop transmission based on FM-EDFA is shown in Fig. 1(a). OAM_{+1} mode is generated after loading phase pattern on spatial light modulator (SLM). Two spatial modes (LP_{01} and OAM_{+1}) fields are transmitted in parallel after beam splitter (BS). A FM-EDFA (only supporting three modes: LP_{01}, OAM_{+1} and OAM_{-1}, where $\mathrm{OAM}_{\pm 1} = \mathrm{LP}_{11\mathrm{a}} \pm \mathrm{j} * \mathrm{LP}_{11\mathrm{b}}$) is employed at the relay. At the input end of the relay, the signal and background fields are coupled into few-mode fiber

Manuscript received 11 May 2022; revised 29 June 2022; accepted 14 July 2022. Date of publication 19 July 2022; date of current version 5 August 2022. This work was supported in part by the National Natural Science Foundation of China under Grants 61801043 and 62075017 and in part by the Fund of State Key Laboratory of IPOC under Grant IPOC2021ZT19, China. *(Corresponding author: Shanyong Cai.)*

The authors are with the State Key Laboratory of Information Photonics and Optical Communications, Beijing University of Posts and Telecommunications, Beijing 100876, China (e-mail: cbb0528@bupt.edu.cn; caishanyong@bupt.edu.cn; zhangzhiguo@bupt.edu.cn).

Digital Object Identifier 10.1109/JPHOT.2022.3192449

This work is licensed under a Creative Commons Attribution-NonCommercial-NoDerivatives 4.0 License. For more information, see https://creativecommons.org/licenses/by-nc-nd/4.0/

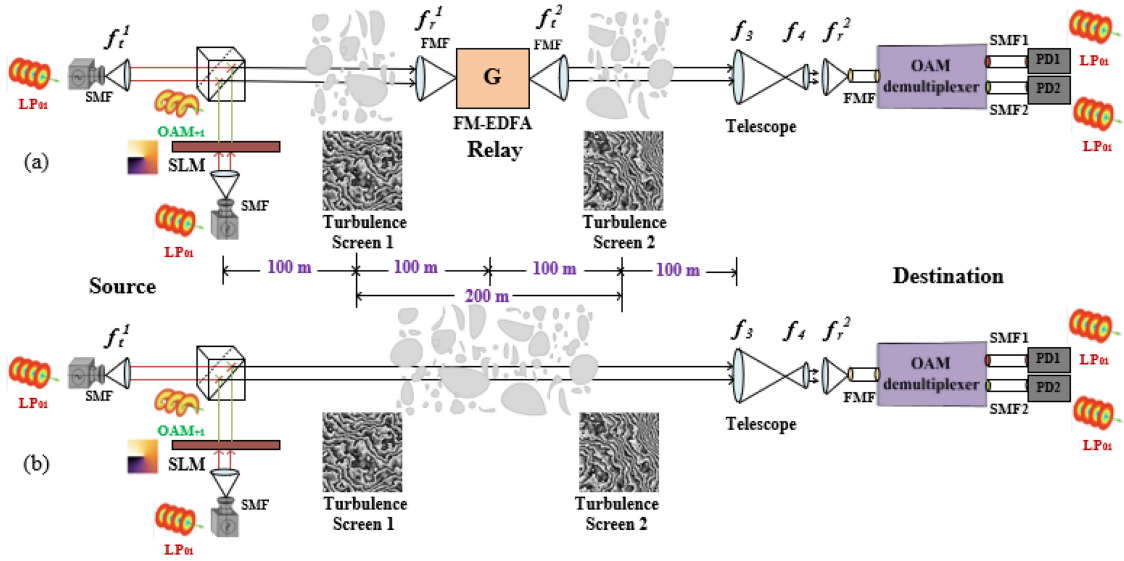

Fig. 1. The diagrams of (a) the dual-hop all-optical relaying system based on FM-EDFA, (b) the single-hop system.

TABLE I
LINK PARAMETERS

	Transmitting lens focal length		Telescope focal length		Receiving lens focal length	
The dual-hop system	First hop f_t^1	Second hop f_t^2	f_3	f_4	First hop f_r^1	Second hop f_r^2
	20cm	21.15cm	30cm	3cm	21.5cm	1.8cm
The single-hop system	20cm				2.1cm	

(FMF) pigtails of FM-EDFA through the receiving lens and are amplified and forwarded to the destination. The FMF is taken to be graded-index fiber, with profile parameter $\rho = 2$, thus the spatial distribution of core mode in the FMF is given by

$$\psi_{m,n}(r,\theta) = C * L_{n-1}^{m}\left(\frac{r^2}{w^2}\right) * \left(\frac{r}{w}\right)^{m} * e^{\left(-\frac{r^2}{2w^2}\right)} * \begin{cases} e^{jm\theta} \\ e^{-jm\theta}, \end{cases} \tag{1}$$

where C is the amplitude constant, L_n^m are the associated Laguerre polynomials, and w is a constant relating modal diameter. Here, w is set to 3.89 μm, so the mode field diameter of LP_{01} mode is 11 μm which is equal to that of OFS' FMFs. At the destination, firstly, the beam diameter is reduced to one-tenth through a telescope. Secondly, different OAM mode fields are demultiplexed by the OAM mode demultiplexer [14] and are demodulated separately by blind detection algorithm [15].

As a contrast, the single-hop SDM FSO system is depicted in Fig. 1(b). It makes no difference from the dual-hop system in structure except for the lack of a relay. The LP_{01} and OAM_{+1} mode fields are received directly at the destination. The BER performance of the two systems will be compared under the same turbulence level and transmission power.

The total link length is 400 m. Two turbulence screens simulating atmospheric turbulence in 200 m free space are fixed at 100 m and 300 m away from the source respectively. The relay is placed in the middle of the link by default. Other link parameters after optimizing the coupling efficiency are shown in Table I.

B. Channel Model

The operating wavelength is 1550 nm. $\alpha_i = L_i * |h_i|^2$ indicates the total channel impairment of the ith hop. The path loss L_i and the small-scale fading gain h_i play decisive roles in the temporal random atmospheric channel impairment. $L_i\,(dB) = a_{attn} * d_i$ where a_{attn} denotes the weather-dependent attenuation coefficient whose value is usually $-0.43\,dB/km$ under clear air and d_i denotes the length of the i th hop. h_i is turbulence-induced random coefficient and will be obtained by simulating AT in the link. AT is simulated by moving and scanning large turbulence screens generated by Fourier Transform method [16]. In the scheme, to ensure fair comparison, turbulence screens used in the dual-hop and single-hop FSO systems are the same for the same turbulence intensity.

D/r_0 is used to characterize the effect of atmospheric turbulence. $D = 38\,mm$ is the transmitting beam diameter. r_0 is the atmospheric coherence length, a parameter describing the turbulence strength [17] and can be approximated by

$$r_0 = \left(0.432 C_n^2 k^2 d\right)^{-\frac{3}{5}},\ l_0 \le r_0 \le L_0, \tag{2}$$

where k is the wave number and d is the transmission distance. C_n^2 is the refractive index structure constant. The value of r_0 changes with the change of C_n^2. $C_n^2 = 1 \times 10^{-15}$, 4×10^{-15}, 7×10^{-15}, 1×10^{-14} and 2×10^{-14} are applied respectively in the simulation.

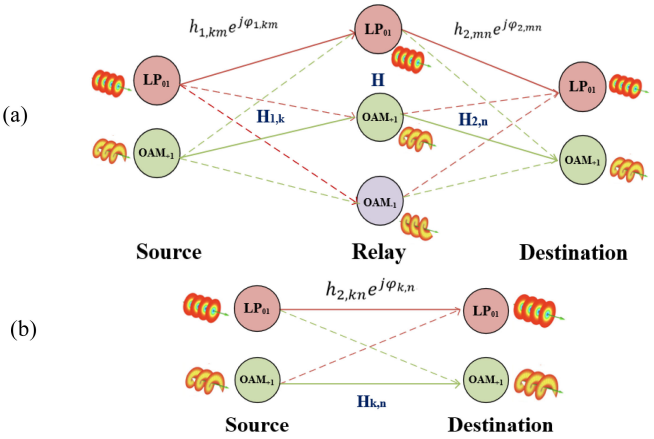

Fig. 2. The transmission model diagrams of (a) the dual-hop system, (b) the single-hop system.

III. SDM FSO System Model

In this section, we develop models for the dual-hop and single-hop SDM FSO system. Systems employ intensity modulation-direct detection (IM/DD) with on-off keying (OOK). These models are based on the approach introduced in [14].

A. Dual-Hop Transmission Model With Relay

The diagram of the dual-hop model with FM-EDFA based relay oriented to SDM FSO system is shown in Fig. 2(a). At the relay, the received electric field is composed of signal and background radiation electric field. The amplification gain at FM-EDFA is fixed to keep the average output power $P_r = 2P_t$, where P_t is the transmitting power of each mode. The amplification gain is given by

$$G = \frac{P_r + 3n_{sp}hv_0B_0}{P_t\left(\sum_{k=1}^{2}\sum_{m=1}^{3}E\left[\alpha_{1,km}\right]\right) + 3P_b + 3n_{sp}hv_0B_0}, \tag{3}$$

where n_{sp} is the amplifier spontaneous emission factor, h is the Planck's constant, v_0 is the optical center frequency, B_0 is the optical bandwidth of the system, and $n_{sp}hv_0B_0$ represents the ASE noise power. P_b is the background radiation power. Moreover, $k = 1,\ 2$ denote LP_{01} and OAM_{+1} mode of the source, respectively. $m = 1,\ 2,\ 3$ denote LP_{01}, OAM_{+1} and OAM_{-1} mode of the FM-EDFA, respectively. $E[\alpha_{1,km}]$ is the average channel impairment of the first hop with $\alpha_{1,km} = L_{km}*|h_{km}|^2$. Due to the first hop length is just 200 *m* by default, the amplification gain of each mode is less than 3 dB when *Cn*2 is in the order of 1E-14 or 1E-15. Thus, the magnification required is small for each mode, and the impact of mode dependent gain is negligible. At the destination, photodetector (PD) is utilized to convert optical signals to photocurrent. The electric field, photocurrent after PD, and various noise variances at the destination are as follows.

1) Electric Field: At the destination, $n = 1,\ 2$ denote LP_{01} and OAM_{+1} mode channel respectively. The total electric field of the nth mode $E_{d,n}(t) = E_S(\mathrm{t}) + E_b(\mathrm{t}) + E_{ASE}(\mathrm{t})$, represents the sum of signal electric field, background radiation electric field and the ASE electric field.

Signal Electric Field:

$$E_S\left(\mathrm{t}\right) = \sum_{k=1}^{2}\sqrt{2x_kP_t}\left|H_{1,k}HH_{2,n}^T\right|\cos\left(w_0t + \varphi_{s,k,n}\right), \tag{4}$$

where $H_{1,k} = \left[h_{1,k1}e^{j\varphi_{1,k1}}, h_{1,k2}e^{j\varphi_{1,k2}}, h_{1,k3}e^{j\varphi_{1,k3}}\right]$ and $H_{2,n} = \left[h_{2,1n}e^{j\varphi_{2,1n}}, h_{2,2n}e^{j\varphi_{2,2n}}, h_{2,3n}e^{j\varphi_{2,3n}}\right]$ are the channel fading vectors of the first and the second hop, respectively. $h_{1,km}e^{j\varphi_{1,km}}$ is the fading coefficient from the kth mode of the source to the mth fiber mode of FM-EDFA in the first hop. Similarly, $h_{2,mn}e^{j\varphi_{2,mn}}$ is the fading coefficient from the mth mode of FM-EDFA to the nth mode of destination in the second hop. The amplification matrix of FM-EDFA is expressed as

$$H = \begin{pmatrix} \sqrt{G} & 0 & 0 \\ 0 & \sqrt{G} & 0 \\ 0 & 0 & \sqrt{G} \end{pmatrix}. \tag{5}$$

$H_{1,k}HH_{2,n}^T = \sum_{m=1}^{3}h_{1,km}e^{j\varphi_{1,km}}\sqrt{G}h_{2,mn}e^{j\varphi_{2,mn}}$ represents the total channel fading coefficient.

Background Radiation Electric Field: The background radiation electric field E_b is composed of the relay background radiation electric field $E_{b,r}$, and the destination background radiation electric field $E_{b,d}$. The expression is given by

$$\begin{aligned} E_b\left(\mathrm{t}\right) &= E_{b,r}\left(\mathrm{t}\right) + E_{b,d}\left(\mathrm{t}\right) \\ &= \sum_{m=1}^{3}\sqrt{2N_b\delta_vG}\sum_{l=-M}^{M}h_{2,mn}\cos\left(w_lt + \varphi_{r,l,m,n}\right) \\ &\quad + \sqrt{2N_b\delta_v}\sum_{l=-M}^{M}\cos\left(w_lt + \varphi_{d,l,n}\right), \end{aligned} \tag{6}$$

where $N_b = P_b/B_0$ denotes the background radiation power spectral density, δ_v is the spacing of the considered frequencies, and $w_l = w_0 + 2\,\pi w_0 l\delta_0$ with $w_0 = 2\pi v_0$.

ASE electric field:

$$\begin{aligned} E_{ASE}\ \left(\mathrm{t}\right) &= \sum_{m=1}^{3}\sqrt{2N_a\delta_v}h_{2,mn} \\ &\quad \times \sum_{l=-M}^{M}\cos\left(w_lt + \varphi_{ASE,l,m,n}\right), \end{aligned} \tag{7}$$

where $N_a = n_{sp}\ (G-1)hv_0$ is the spectral density of the ASE noise. In the above equations, $\varphi_{s,k,n}$, $\varphi_{r,l,m,n}$, $\varphi_{d,l,n}$ and $\varphi_{ASE,l,m,n}$ are the mutually independent random phases.

Finally, after PD, the optical signal is converted into electrical signal. The expression of the photocurrent is $I_{photon} = R*E_{d,n}^2$, where R is the responsivity of PD. Following the approach in [13], the direct current terms and beat noise terms can be obtained by inserting the expression of $E_{d,n}$ into I_{photon}.

2) Direct Current: The signal current in the nth mode of the destination is expressed as

$$I_{s,n} = R*E_{s,n}^2 = RP_t\left(\sum_{k=1}^{2}x_k\left|H_{1,k}HH_{2,n}^T\right|^2\right). \tag{8}$$

Similarly, the relay background-background direct current, the destination background-background direct current, and the ASE-ASE direct current are respectively expressed as

$$I_{b\times b,rn} = RN_bB_0G\left(\sum_{m=1}^{3} {h_{2,mn}}^2\right), \tag{9}$$

$$I_{b\times b,dn} = RN_bB_0, \tag{10}$$

$$I_{ASE\times ASE,n} = RB_0N_a\left(\sum_{m=1}^{3} {h_{2,mn}}^2\right). \tag{11}$$

3) Noise Variance: The noises considered include beat noises when squaring the electric field, shot noise caused by electron emission inhomogeneity, and thermal noise of PD.

Background-Background Beat Noise: The variance of the background-background beat noise $\sigma^2_{b\times b,n}$, is the sum of the variance of the relay background-background radiation beat noise $\sigma^2_{b\times b,rn}$, the destination background-background radiation beat noise $\sigma^2_{b\times b,dn}$, and the relay-destination background beat noise $\sigma^2_{rb\times db,n}$. Their expressions are respectively given by

$$\sigma^2_{b\times b,rn} = R^2\ N_b^2\left(2B_eB_0 - B_e^2\right) \times\left(G^2\sum_{m=1}^{3} h_{2,mn}^4 + 4\sum_{i=1}^{3}\sum_{j=1,j\neq i}^{3} G_iG_j{h_{2,in}}^2{h_{2,jn}}^2)\right), \tag{12}$$

$$\sigma^2_{b\times b,dn} = R^2\ N_b^2\left(2B_eB_0 - B_e^2\right), \tag{13}$$

$$\sigma^2_{rb\times db,n} = 4R^2\ N_b^2G\left(2B_eB_0 - B_e^2\right)\left(\sum_{m=1}^{3} {h_{2,mn}}^2\right). \tag{14}$$

ASE-ASE Beat Noise:

$$\sigma^2_{ASE\times ASE,n} = R^2\ \left(2B_eB_0 - B_e^2\right) \times\left(N_a^2\sum_{m=1}^{3} {h_{2,mn}}^4 + 4\sum_{i=1}^{3}\sum_{j=1,j\neq i}^{3} N_{a,i}N_{a,j}{h_{2,in}}^2{h_{2,jn}}^2)\right). \tag{15}$$

Background-Signal Beat Noise: The background-signal beat noise $\sigma^2_{b\times s,n}$ includes the relay background-signal beat noise $\sigma^2_{b\times s,rn}$ and the destination background-signal beat noise $\sigma^2_{b\times s,dn}$. Their variances are respectively given by

$$\sigma^2_{b\times s,rn} = 4R^2\ P_tN_bB_eG\left(\sum_{k=1}^{2} x_k\left|H_{1,k}HH_{2,n}^T\right|^2\right) \times\left(\sum_{m=1}^{3} h_{2,mn}^2\right), \tag{16}$$

$$\sigma^2_{b\times s,dn} = 4R^2\ P_tN_bB_e\left(\sum_{k=1}^{2} x_k\left|H_{1,k}HH_{2,n}^T\right|^2\right). \tag{17}$$

$$\sigma^2_{b\times s,n} = \sigma^2_{b\times s,rn}\ + \sigma^2_{b\times s,dn} = 4R^2P_tN_bB_e\left(\sum_{k=1}^{2} x_k\left|H_{1,k}HH_{2,n}^T\right|^2\right) \times\left(1 + G\sum_{m=1}^{3} {h_{2,mn}}^2\right). \tag{18}$$

Background-ASE Beat Noise: Similar to the background–signal beat noise, the background-ASE beat noise consists of the relay background-ASE beat noise and the destination background- ASE beat noise. The variance is expressed as

$$\sigma^2_{b\times ASE,n} = 4R^2N_bN_a\left(2B_eB_0 - B_e^2\right)\left(\sum_{m=1}^{3} {h_{2,mn}}^2\right) \times\left(1 +\ G\sum_{m=1}^{3} {h_{2,mn}}^2\right). \tag{19}$$

Signal-ASE Beat Noise:

$$\sigma^2_{s\times ASE,n} = 4R^2P_tB_eN_a\left(\sum_{k=1}^{2} x_k\left|H_{1,k}HH_{2,n}^T\right|^2\right) \times\left(\sum_{m=1}^{3} {h_{2,mn}}^2\right). \tag{20}$$

Shot Noise: For transmitted symbol $x = 0$ and $x = 2$, the shot noise variances $\sigma^2_{shot,off,n}$ and $\sigma^2_{shot,on,n}$ are given by

$$\sigma^2_{shot,off,n} = 2q\left(I_{b\times b,rn} + I_{b\times b,dn} + I_{ASE\times ASE,n}\right)B_e, \tag{21}$$

$$\sigma^2_{shot,on,n} = \sigma^2_{shot,off,n}\ + 2qI_{s,n}B_e. \tag{22}$$

Thermal Noise:

$$\sigma^2_{th} = \frac{4KTB_e}{R_L}, \tag{23}$$

where K is the Boltzmann constant, T is the temperature in Kelvin, and R_L is the photodetector load resistance.

Above all, for $x = 0$ and $x = 2$, the total noise variance of the dual-hop system $\sigma^2_{off,n}$ and $\sigma^2_{on,n}$ are respectively expressed as

$$\sigma^2_{off,n} = \sigma^2_{b\times b,n} + \sigma^2_{ASE\times ASE,n} + \sigma^2_{b\times ASE,n} + \sigma^2_{shot,off,n} + \sigma^2_{th}, \tag{24}$$

$$\sigma^2_{on,n} = \sigma^2_{off,n}\ + 2qI_{s,n}B_e + \sigma^2_{b\times s,n} + \sigma^2_{s\times ASE,n}. \tag{25}$$

Finally, the signal current in (8) and the noise variances in (24) – (25) constitute the model for dual-hop SDM FSO system.

B. Single-Hop Transmission Model

The transmission diagram of the single-hop SDM FSO system is shown in Fig. 2(b). The expressions of electric field, direct current, and noise variances are as follows.

1) Electric Field: The destination electric field is composed of signal and background electric field, given by

$$E_{d,n}(t) = E_{S,n}(\mathrm{t}) + E_{b,d}(\mathrm{t})$$

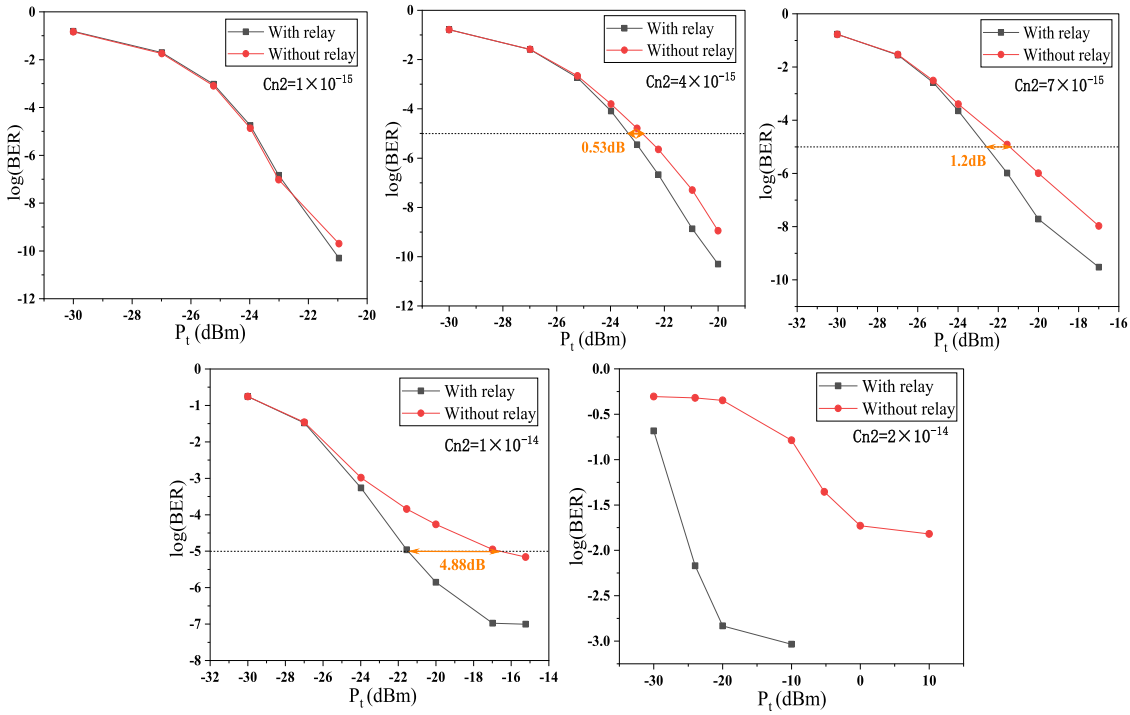

Fig. 3. The BER under $C_n^2 = 1\times10^{-15}, 4\times10^{-15}, 7\times10^{-15}, 1\times10^{-14}$ and 2×10^{-14}, respectively.

$$= \sum_{k=1}^{2} \sqrt{2x_k P_t}\,|H_{k,n}|\cos\left(w_0 t + \varphi_{k,s,n}\right)$$

$$+ \sqrt{2N_b\delta_v} \sum_{l=-M}^{M} \cos\left(w_l t + \varphi_{d,l,n}\right). \quad (26)$$

2) Direct Current: The signal direct current and background-background direct current of the nth mode after PD are respectively given by

$$I_{s,n} = R{*}\, E_{d,n}^2 = RP_t \left(\sum_{k=1}^{2} x_k |H_{k,n}|^2\right), \quad (27)$$

$$I_{b\times b,dn} = RN_b B_0. \quad (28)$$

3) Noise Variance: The beat noises include background-background beat noise and background-signal beat noise, their variances are respectively given by

$$\sigma_{b\times b,dn}^2 = R^2\, N_b^2 \left(2B_e B_0 - B_e^2\right), \quad (29)$$

$$\sigma_{b\times s,dn}^2 = 4R^2 P_t N_b B_e \left(\sum_{k=1}^{2} x_k |H_{k,n}|^2\right). \quad (30)$$

For transmitting symbol $x = 0$ and $x = 2$, the shot noise variances $\sigma_{shot,off,h}^2$ and $\sigma_{shot,on,h}^2$ are given by

$$\sigma_{shot,off,n}^2 = 2q\left(I_{b\times b,rn} + I_{b\times b,dn}\right)B_e, \quad (31)$$

$$\sigma_{shot,on,n}^2 = \sigma_{shot,off,n}^2 + 2qI_{s,n}B_e. \quad (32)$$

TABLE II
SYSTEM PARAMETERS

Parameter	Value
Wavelength (λ)	1550 *nm*
Electrical bandwidth (B_e)	2 *GHz*
Optical bandwidth (B_0)	125 *GHz*
Data rate (R_b)	2 *Gbps*
Amplifier spontaneous factor (n_{sp})	1.4
Receiver noise temperature (T)	300 *K*
Receiver quantum efficiency (ρ)	0.75
Photodetector load resistance (R_L)	50 Ω
Background radiation energy (N_b)	1.6×10^{-19} *W/Hz*

In summary, for transmitted symbol $x = 0$ and $x = 2$, the total noise variances $\sigma_{off,n}^2$ and $\sigma_{on,n}^2$ are expressed as

$$\sigma_{off,n}^2 = \sigma_{b\times b,n}^2 + \sigma_{shot,off,n}^2 + \sigma_{th}^2, \quad (33)$$

$$\sigma_{on,n}^2 = \sigma_{off,n}^2 + 2qI_{s,n}B_e + \sigma_{b\times s,n}^2, \quad (34)$$

where σ_{th}^2 denotes the thermal noise of PD. In general, the single-hop transmission system is composed of signal current in (27) and the noise variances in (33)–(44).

IV. NUMERICAL RESULTS

In this section, the BER performance of the above two systems are analyzed, with the simulation parameters shown in Table II. The BER is averaged over 10000 different fading states. The bit rate of the system is 2 *Gbps*. Assuming that

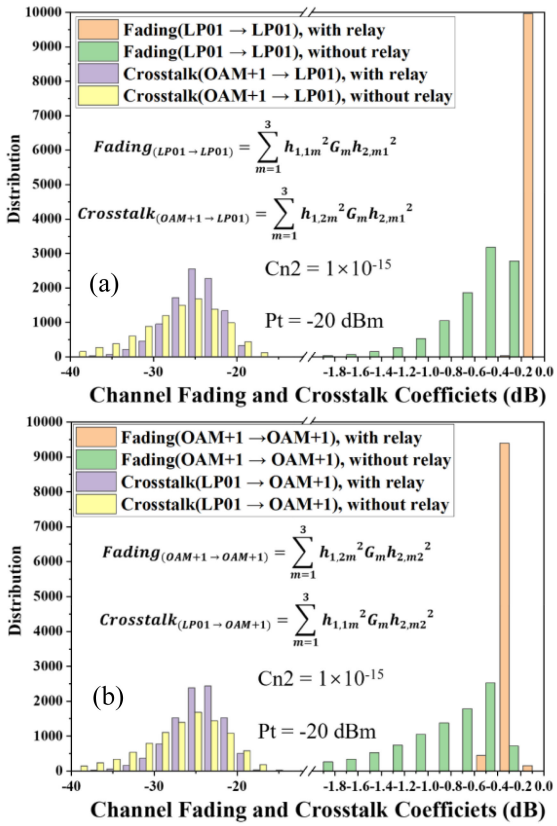

Fig. 4. The channel fading and crosstalk coefficients of $C_n^2 = 1 \times 10^{-15}$.

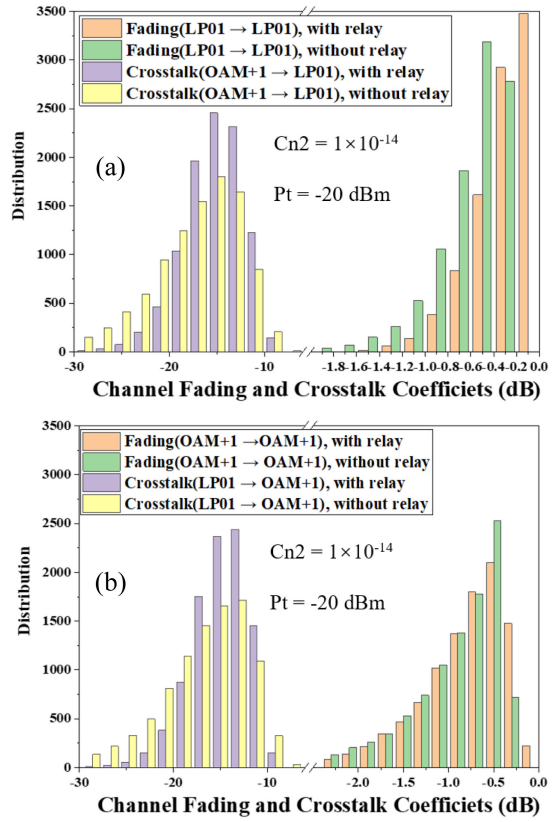

Fig. 5. The channel fading and crosstalk coefficients of $C_n^2 = 1 \times 10^{-14}$.

the turbulence state changes every $1ms$, each fading state corresponds to 2E6 bits. Fig. 3 shows the BER when the refractive index structure constant (C_n^2) is $1 \times 10^{-15}, 4 \times 10^{-15}, 7 \times 10^{-15}, 1 \times 10^{-14}$ and 2×10^{-14}. Obviously, regardless of the turbulence level, the BER performance of the dual-hop system is better than that of the single-hop system. With the increase of turbulence intensity, the advantages of dual-hop system based on FM-EDFA are more obvious. To achieve the same BER $= 1 \times 10^{-5}$, the power budget is increased by 0.53 dB, 1.2 dB, and 4.88 dB, when $C_n^2 = 4 \times 10^{-15}, 7 \times 10^{-15}$ and 1×10^{-14}, respectively. The reason is that relay-assisted transmission can exploit the distance-dependency of the log-amplitude variance of the atmospheric fading in FSO system [6].

However, as the turbulence continues to increase $(C_n^2 = 2 \times 10^{-14})$, the dual-hop system cannot achieve an ideal BER either, although it still outperforms the single-hop system. Moreover, when $C_n^2 = 3 \times 10^{-14}$, the minimum BER that the dual-hop system can achieve is just 0.057. The main reason is inter-mode crosstalk.

To investigate the effect of inter-mode crosstalk on BER, the channel fading and crosstalk coefficients for 10000 turbulent states are calculated under $P_t = -20\,dBm$. The coefficient distributions of $C_n^2 = 1 \times 10^{-15}$ and 1×10^{-14} are respectively shown in Figs. 4 and 5. Take the LP_{01} mode (Figs. 4(a) and 5(a)) for example, the channel fading coefficient is characterized by $\delta = \sum_{m=1}^{3} |h_{1,1m}{}^2 G h_{2,m1}{}^2|$, representing the received LP_{01} mode field at destination transmitted from LP_{01} mode at source. The crosstalk coefficient is characterized by $\varepsilon = \sum_{m=1}^{3} |h_{1,2m}{}^2 G h_{2,m1}{}^2|$, representing the crosstalk from the signal carried in OAM_{+1} mode at the source to the signal carried in LP_{01} mode at the destination. Similarly, Figs. 4(b) and 5(b) shows the distributions of channel fading and crosstalk coefficients of OAM_{+1} mode field. Apparently, the dual-hop system has larger channel transmission coefficients and less crosstalk for both modes. Moreover, by comparing Figs. 4 and 5, it is confirmed that the crosstalk among modes increases with the enhancement of atmospheric turbulence, which is the main factor affecting the BER. Moreover, they show that the variance of the crosstalk coefficient distribution of the single hop system is large, thus contains more strong crosstalk components.

Furthermore, the optimal placement of relay is explored under $C_n^2 = 1 \times 10^{-14}$. To discuss the effect of position of relay on BER performance accurately, 8 turbulence screens are uniformly distributed on the transmission path. Each turbulence screen simulates atmospheric turbulence of 50 m free space, and fixed at S_i m ($S_i = 25 + i * 50, i = 01,2 \ldots 7$) from the source in sequence. The BER is numerically calculated when the relay is placed at $d_1 = 50$ m, 100 m…350 m, respectively. Results show that the BER performance is the best when $d_1 = 150$ m, followed by $d_1 = 50$ m and 100 m (Fig. 6). And the BER is the worst when $d_1 = 300$ m and 350 m. In general, the BER performance is better when the relay is placed slightly near the source.

Moreover, FM-EDFA based relay amplifies and forwards different modes of light separately in SDM FSO systems, a process that can be analogous to parallel relaying transmission. The simulation result is consistent with [8], which

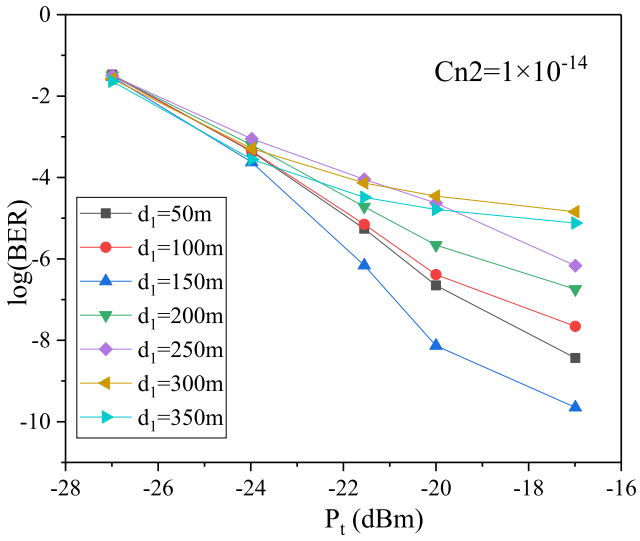

Fig. 6. The BER of different relay placements.

proved that parallel relays should be placed close to the source. It can demonstrate, to some extent, the plausibility of our results.

V. Conclusion

In this paper, we employ relay assisted transmission in space division multiplexing FSO system to resist atmospheric turbulence, thereby reducing inter-mode crosstalk and improving the BER performance. An accurate dual-hop model based on a FM-EDFA is proposed. Simulation results show that the dual-hop system outperforms the single-hop system. The stronger the turbulence, the more significant the advantage of the relaying system. In addition, the crosstalk can be further suppressed by descrambling DSP algorithm or increasing the interval among modes in the future work to reduce the BER of the system. The combination of huge transmission capacity and excellent BER performance makes SDM system with FM-EDFA based relays attractive in the future last-mile FSO communications.

References

[1] T. Tolker-Nielsen, B. Demelenne, and E. Desplats, "In-orbit test results of the first SILEX terminal," *Free-Space Laser Commu. Technol. XI*, vol. 3615, pp. 31–42, Apr. 1999.

[2] X. Zhu and J. M. Kahn, "Free-space optical communication through atmospheric turbulence channels," *IEEE Trans. Commun.*, vol. 50, no. 8, pp. 1293–1300, Aug. 2002.

[3] X. Zhu and J. Kahn, "Performance bounds for coded free-space optical communications through atmospheric turbulence channels," *IEEE Trans. Commun.*, vol. 51, no. 8, pp. 1233–1239, Aug. 2003.

[4] X. Zhu and J. Kahn, "Markov chain model in maximum-likelihood sequence detection for free-space optical communication through atmospheric turbulence channels," *IEEE Trans. Commun.*, vol. 51, no. 3, pp. 509–516, Mar. 2003.

[5] E. G. Larsson, O. Edfors, F. Tufvesson, and T. L. Marzetta, "Massive MIMO for next generation wireless systems," *IEEE Commun. Mag.*, vol. 52, no. 2, pp. 186–195, Feb. 2014.

[6] M. Safari and M. Uysal, "Relay-assisted free-space optical communication," *IEEE Trans. Wireless Commun.*, vol. 7, no. 12, pp. 5441–5449, Dec. 2008.

[7] S. Kazemlou, S. Hranilovic, and S. Kumar, "All-optical multihop free space optical communication systems," *J. Lightw. Technol.*, vol. 29, no. 18, pp. 2663–2669, Sep. 2011.

[8] M. A. Kashani, M. Safari, and M. Uysal, "Optimal relay placement and diversity analysis of relay-assisted free-space optical communication systems," *J. Opt. Commun. Netw.*, vol. 5, pp. 37–47, 2013.

[9] N. Bai, E. Ip, T. Wang, and G. Li, "Multimode fiber amplifier with tunable modal gain using a reconfigurable multimode pump," *Opt. Exp.*, vol. 19, pp. 16601–16611, 2011.

[10] N. Bai et al., "Mode-division multiplexed transmission with inline few-mode fiber amplifier," *Opt. Exp.*, vol. 20, pp. 2668–2680, 2012.

[11] G. Li, N. Bai, N. Zhao, and C. Xia, "Space-division multiplexing: The next frontier in optical communication," *Adv. Opt. Photon.*, vol. 6, pp. 413–487, 2014.

[12] B. Huang et al., "Turbulence-resistant free-space optical communication using few-mode preamplified receivers," in *Proc. Eur. Conf. Opt. Commun.*, 2017, pp. 1–3.

[13] S. Cai, Z. Zhang, and X. Chen, "Turbulence-resistant all optical relaying based on few-mode EDFA in free-space optical systems," *J. Lightw. Technol*, vol. 37, no. 9, pp. 2042–2049, May 2019.

[14] N. Wang et al., "Erbium-doped fiber amplifier for OAM modes using an annular-core photonic lantern," in *Proc. Conf. Lasers Electro-Opt.*, 2017, Paper STu4K.4.

[15] M. L. B. Riediger, R. Schober, and L. Lampe, "Blind detection of on-off keying for free-space optical communications," in *Proc. Can. Conf. Electro-Opt. Eng.*, 2008, pp. 1361–1364.

[16] X. Tong et al., "Simulating atmospheric turbulence using a spatial light modulator based on Fourier transform," in *Proc. Conf. Lasers Electro-Opt. - Laser Sci. Photon. Appl.*, 2014, Paper SM4J.3.

[17] L. C. Andrews and R. L. Phillips, *Laser Beam Propagation Through Random Media*, 2nd ed. Bellingham, WA, USA: SPIE, 2005.